

## HEAT-DRIVEN ADSORPTION CHILLER SYSTEMS FOR SUSTAINABLE COOLING APPLICATIONS

*Patrick Ruch<sup>a</sup>, Sarmenio Saliba<sup>a</sup>, Chin Lee Ong<sup>a</sup>, Yazid Al-Shehr<sup>b</sup>, Abdalrahman Al-Rihail<sup>b</sup>, Ahmed Al-Mogbel<sup>b</sup>, and Bruno Michel<sup>a</sup>*

*<sup>a</sup> IBM Research – Zurich, Säumerstrasse 4, 8803 Rüschlikon, Switzerland*

*<sup>b</sup> King Abdulaziz City for Science and Technology (KACST), Riyadh 11442, Saudi Arabia*

**Abstract:** Thermally driven adsorption chillers enable utilization of low-grade heat below 100°C to drive refrigeration cycles at minimum electrical energy consumption. Therefore, this technology is crucial to enable waste heat usage and substantially cut the power drawn from electrical grids and thereby improve the energy efficiency of air-conditioning infrastructure. Two scenarios for the implementation of adsorption heat pumps are considered: (i) hot-water cooled datacenters and (ii) solar cooling. Simulation studies reveal distinct operating windows for the adsorption chiller in each application and, accordingly, the need for adsorbent materials tailored to the desired temperature lift to optimally use the driving heat. Adsorption experiments were carried out in a custom-built apparatus to quantify the cooling power per unit mass of adsorbent and its thermal response in relation to the applied temperature swing. The results reveal poor adsorbent utilization in present adsorption chillers due to a mismatch between the adsorption characteristics of the adsorbent and the boundary conditions of the application as well as incomplete thermal cycling of the adsorbent due to poor heat transport.

**Key Words:** adsorption, solar energy, datacenter, waste heat

### 1 INTRODUCTION

Space heating and cooling account for over one-third of energy consumption in buildings, which in turn are responsible for more than one-third of global energy consumption [1]. By 2050, the cooling loads in hot developing countries will increase rapidly between three- and more than six-fold resulting in a severe surge in electricity demand for cooling which already accounts for more than 70% of domestic electricity consumption in hot countries during peak demand [1, 2] In the course of the 21<sup>st</sup> century, it is likely that the share of cooling of the total space-conditioning CO<sub>2</sub> emissions will rise from 5% in 2000 to more than 70% by 2100 [3]. As a result, there is a strong need for efficient cooling technologies with minimal electricity consumption and CO<sub>2</sub> footprint in order to provide a sustainable air-conditioning infrastructure, particularly in hot countries.

The abundance of low-grade heat from industrial processes [4] and solar heat [5] motivates the use of thermally driven heat pumps [6] for air-conditioning applications. Adsorption heat pumps rely on the reversible physisorption of a refrigerant vapor, the adsorptive, on a porous material, the adsorbent [7]. The adsorption refrigeration cycle is driven mainly by temperature swings applied to the adsorbent, thus requiring minimal amounts of electricity to operate. Further, water can be readily used as an environmentally benign and highly effective refrigerant due to its excellent latent heat of vaporization per unit volume and mass [8]. Therefore, adsorption cooling is a promising technology to make use of low-grade heat from sustainable energy sources aimed at reducing electricity peaks for air-conditioning.

In contrast to vapor compression cooling, the adsorbent material in an adsorption chiller assumes a critical role in driving the refrigeration cycle instead of a mechanical compressor.

As will be shown in this contribution, the ideal adsorption characteristics of the adsorbent/adsorptive working pair may vary considerably for different cooling scenarios. Here, two distinct heat-driven cooling applications are investigated by simulation and experiment, namely (i) hot-water cooled datacenters [9] and (ii) solar cooling in desert climate [10].

Using direct water cooling, heat dissipated from servers can be recovered at sufficiently high temperatures to enable free cooling during the entire year, thus eliminating the need for compression cooling and air handling which accounts for 25%-50% datacenter power consumption [9, 11]. With optimized cooling equipment temperature levels are high enough to operate an adsorption chiller [12]. For heterogeneous datacenters consisting of hot-water cooled servers as well as conventional air-cooled IT equipment, improved energy efficiency may be realized through the integration of an adsorption chiller since the heat recovered from the water-cooled servers can be used to provide chilled air for the air-cooled IT infrastructure. Overall, this approach can reduce the energy cost of operating server hardware, which is estimated to account for ca. 25 B\$ of worldwide datacenter spending or about half the yearly expenditure on server hardware [13]. The fraction of power cost increases with the transition to cloud computing due to use of low-cost commodity hardware.

The usage of solar thermal energy for adsorption cooling is an attractive sustainable cooling option in hot countries. In Saudi Arabia, for example, the installed electricity generating capacity is required to double in the timeframe 2007-2017 in order to meet the growth in peak electricity demand, which is primarily governed by air-conditioning needs in summer [14]. Adsorption cooling has the greatest potential for electricity reduction for air-conditioning due to the absence of internal pumps and compressors, leading to a high electrical coefficient of performance ( $COP_{el}$ ). At the same time, the high solar irradiance in hot countries enables high solar thermal collector yields and thus substantial driving power for the adsorption process. However, like all thermally driven cooling technologies, adsorption cooling suffers from a large recooling need which is exacerbated due to the high ambient temperatures in hot countries during cooling season. These conditions differ markedly from the nominal conditions of commercial adsorption chillers, leading to an underutilization of the adsorption capacity and performance degradation. Establishing a better understanding of the operating environment is crucial for the design of improved adsorption systems for solar adsorption cooling in hot climates.

## **2 METHODOLOGY**

### **2.1 System simulation**

Heat-driven adsorption cooling systems using a silica gel/water chiller with 15 kW nominal cooling capacity [15, 16] were implemented in Polysun<sup>®</sup> 5.9 (Vela Solaris, Switzerland). The simulation of server heat usage for adsorption cooling (Figure 1a) assumed a hot-water cooled server rack with nominal outflow temperature of 65°C and a total thermal load of 30 kW/m<sup>2</sup>. In addition, an air-cooled server rack containing storage and network switches with a total thermal load of 10 kW/m<sup>2</sup> was added to the IT hardware configuration. While free cooling can be carried out for the hot-water cooled servers throughout the year by direct heat rejection to ambient in a dry recoler, the air-cooled servers can only make use of free cooling for ambient temperatures lower than 18°C. To test the feasibility of all-year operation without the need for vapor compression cooling, the heat recovered from the water-cooled servers was used to drive the adsorption chiller to charge a chilled water buffer tank. During periods in which elevated ambient temperatures do not allow free cooling for the air-cooled servers, the chilled water from this tank provides the necessary air-conditioning of the rack space. Simulations were carried out for two locations, Munich (Germany) and Dallas, TX

(USA), in order to assess the feasibility of adsorption cooling in the datacenter environment and to identify the operating conditions of the adsorption chiller for these two scenarios.

Solar cooling simulations were performed for a single-family household in Riyadh, Saudi Arabia, with 150 m<sup>2</sup> living area using flat-plate solar thermal collectors (135 m<sup>2</sup> adsorber area) with a hot water buffer (8 m<sup>3</sup> storage volume) to drive the adsorption chiller. Heat rejection was carried out using a dry recoler. Further details of the simulation methodology for the solar cooling scenario can be found in [10].

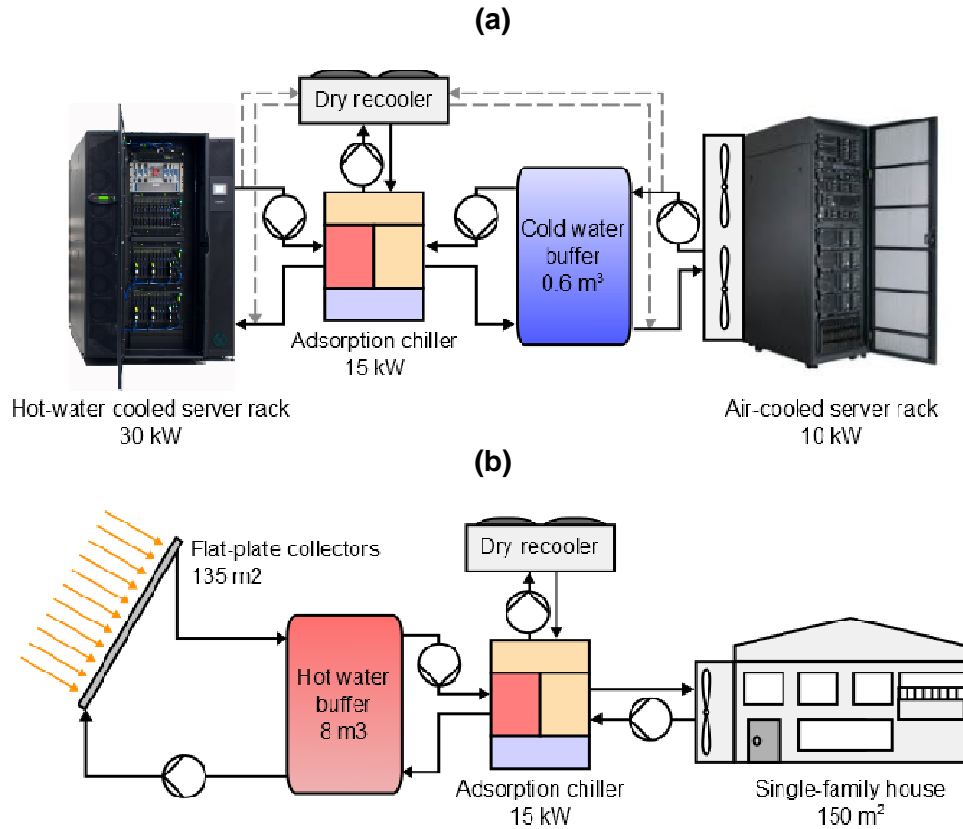


**Figure 1: Simulated heat-driven adsorption cooling scenarios: (a) datacenter waste heat and (b) solar thermal cooling**

## 2.2 Experimental investigation of adsorption characteristics

The adsorption isotherms of water on a micro-/mesoporous silica gel (RD-type, Fuji Silysia, Japan) were measured using a gravimetric sorption analyzer (DVS Vacuum, Surface Measurement Systems, United Kingdom). The adsorption characteristics were interpreted in the context of Dubinin's theory [17] based on the differential molar work of adsorption:

$$A = -RT \ln(p/p_{sat}) \quad (1)$$

where  $R$  is the universal gas constant,  $T$  the temperature of the adsorbent with the corresponding saturation pressure  $p_{sat}(T)$ , and  $p$  is the actual pressure. Using Equation (1), different adsorption states ( $p$ ,  $T$ ) can be compared using the single variable  $A$ .

For measurement of the adsorption dynamics, an in-house experimental setup was used (Figure 2). The apparatus comprises a water-filled evaporator kept at constant temperature and a chamber containing the adsorber heat exchanger. The temperature of the heat

exchanger fluid flowing through the adsorber can be switched between a high temperature ( $T_h$ ) and a medium temperature ( $T_m$ ) reservoir in order to induce adsorption or desorption. The rate of water sorption in g/s was quantified by measuring the flow rate of water vapor using a flow sensor. Multiplication of the mass flow rate by the vaporization enthalpy,  $\Delta_{\text{vap}}H$  in J/g, yielded the cooling power in W. Normalization of the cooling power with respect to the dry adsorbent mass resulted in the specific cooling power (SCP) in W/kg.

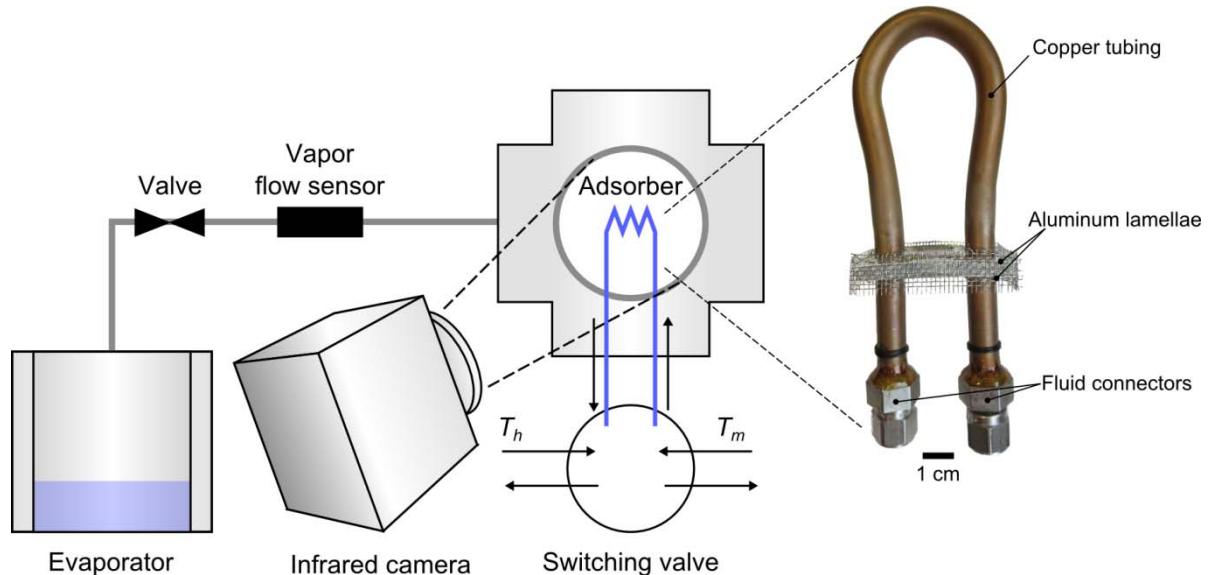


**Figure 2: Experimental scheme for characterization of adsorption rates using thermal swing adsorption with online infrared thermography**

The adsorber heat exchanger used in this work was a tube-lamella heat exchanger unit with two aluminum lamellae (spacing 7 mm) enclosing the silica gel fixed bed adsorbent (Figure 2, right). The diameter of the silica beads was between 1.8 and 2.0 mm and a total dry adsorbent mass of 7.989 g was used. An infrared camera (Silver 420, FLIR Systems Inc., USA) was used to observe the thermal response of the adsorbent during cycling.

### 3 RESULTS AND DISCUSSION

#### 3.1 Adsorption system simulation

The ambient temperatures as well as the water-cooled and air-cooled server temperatures during free cooling operation are plotted in Figure 3 for the two investigated datacenter locations. The shaded areas indicate the temperature span for each of the temperature series. Due to the high outlet temperature of the hot-water cooled servers compared to the ambient temperature, free cooling can be achieved at both locations during the entire year. On the other hand, free cooling for the air-cooled servers was found to be feasible 90% of the time in Munich and only 64% of the time in Dallas due to the higher ambient temperatures of the latter location. In particular, during the months of June to August, no free cooling is possible for the air-cooled servers in Dallas. During this time, all of the thermal energy is dissipated via the cold buffer of the adsorption cooling system (Figure 4). Notably, no vapor compression chiller is needed at either location at any time to provide cooling for the air-cooled servers, as the entire cooling load is provided by the adsorption chiller driven by the waste heat from the hot-water cooled servers.

The cold buffer is useful when the workloads on the water-cooled and air-cooled servers differ substantially. Thus, when no chilled water production is required for air-conditioning of the air-cooled servers, the cold buffer tank is charged to a temperature of 18°C in the top

stratified layer. During maximum chilled water production for air-conditioning, the tank outlet temperature rises up to 18°C in Munich and 22°C in Dallas (Figure 5), which is still low enough to maintain secure operation of the air-cooled IT infrastructure.

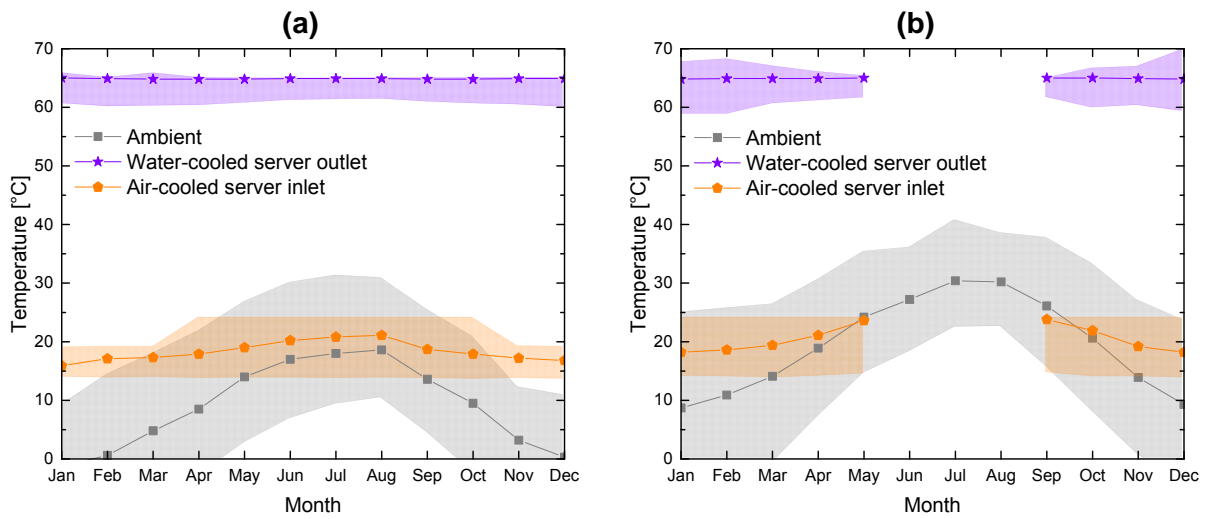


Figure 3: Ambient temperature, water-cooled server outlet temperature and air-cooled server intake temperature for (a) Munich and (b) Dallas

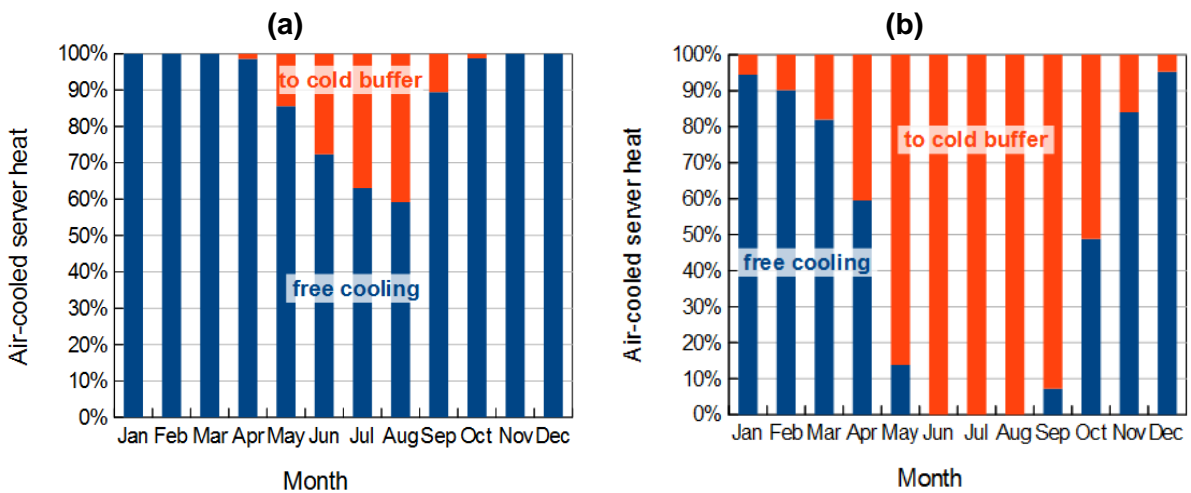


Figure 4: Partitioning of air-cooled server heat dissipation between free cooling and cold buffer for (a) Munich and (b) Dallas.

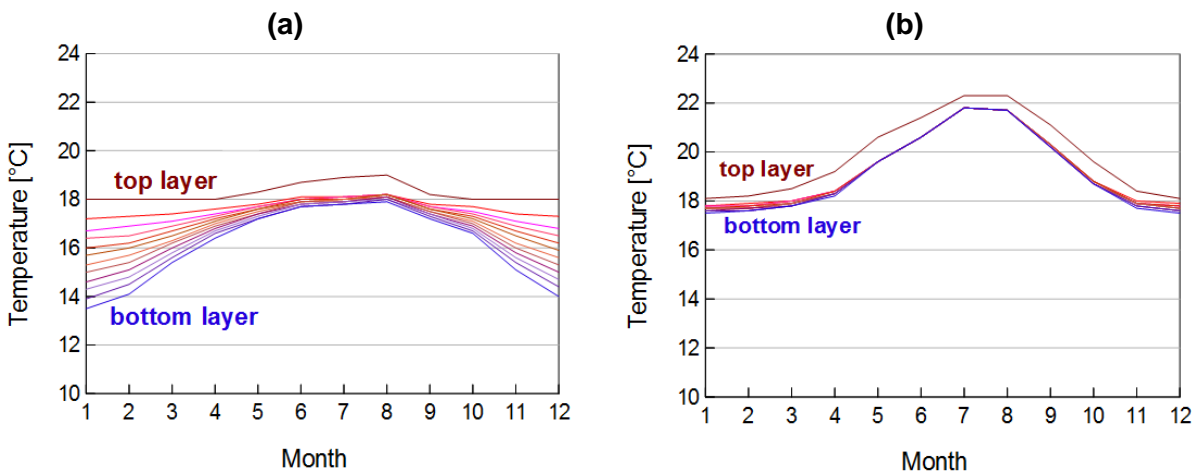
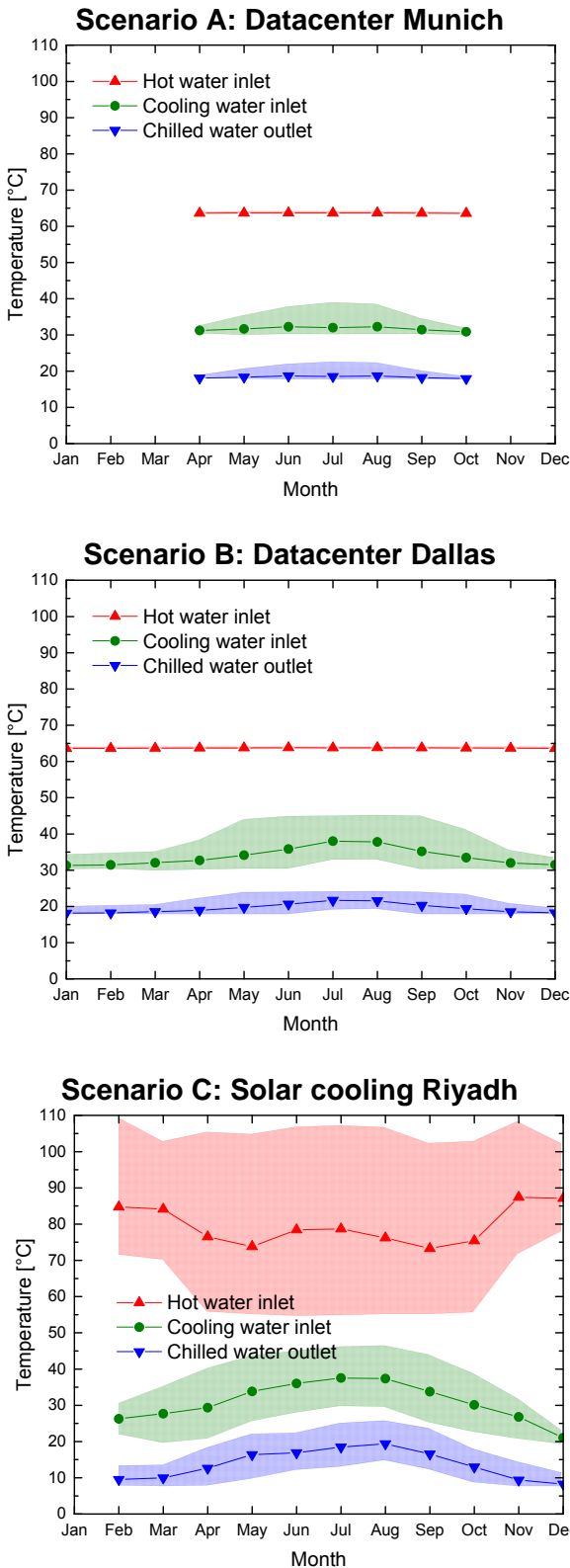


Figure 5: Temperatures of the cold buffer tank stratified layers for (a) Munich and (b) Dallas



**Figure 6: Monthly temperature triples for the three investigated scenarios**

presently implemented 8 m<sup>3</sup> may prove impractical for a single-family home.

The temperature triple comprising the driving temperature  $T_h$ , heat sink temperature  $T_m$  and chilled water temperature  $T_l$  describes the thermodynamic operating conditions of the adsorption chiller. The three scenarios (A) datacenter operation in Munich, (B) datacenter operation in Dallas and (C) solar cooling in Riyadh are compared in terms of their temperature triples in Figure 6. The data points represent the average monthly value while the shaded areas indicate the temperature span for each month.

The yearly average temperature triples  $\{T_h, T_m, T_l\}$  for the three scenarios are  $\{64^\circ\text{C}, 32^\circ\text{C}, 19^\circ\text{C}\}$  for Scenario A,  $\{64^\circ\text{C}, 35^\circ\text{C}, 20^\circ\text{C}\}$  for Scenario B and  $\{77^\circ\text{C}, 35^\circ\text{C}, 17^\circ\text{C}\}$  for Scenario C. The corresponding thermal coefficients of performance ( $\text{COP}_{th}$ ), defined as the ratio of cooling energy to driving energy, were 0.45 (Scenario A), 0.33 (Scenario B) and 0.40 (Scenario C), respectively. The most demanding operation occurs in scenarios B and C during the summer months when the heat sink temperature is highest. The temperature triples in July are  $\{64^\circ\text{C}, 38^\circ\text{C}, 22^\circ\text{C}\}$  with a  $\text{COP}_{th}$  of 0.21 for Scenario B and  $\{79^\circ\text{C}, 38^\circ\text{C}, 18^\circ\text{C}\}$  with a  $\text{COP}_{th}$  of 0.30 for Scenario C. Improved efficiencies can be obtained by exploiting day/night temperature fluctuations in conjunction with a larger cold storage.

The driving temperature in the solar cooling scenario (C) exhibits a substantially larger spread than in the two datacenter scenarios (A, B) due to the large variability in the solar collector yield compared to the workload on the servers. Also, server workloads may be scheduled in a thermally aware manner so as to obtain more uniform heat dissipation in time. The variability in driving temperature for the solar cooling scenario may be minimized by implementing a variable pump speed in the solar loop to target a constant collector outflow temperature or by increasing the size of the hot water buffer. However, a larger hot water buffer than the

### 3.2 Experimental investigation of adsorbent utilization

The adsorption isotherms of water on Fuji RD silica gel at temperatures between 30°C and 70°C are summarized in Figure 7a. According to Dubinin's theorem for microporous adsorbents, the water uptake curves should coincide when plotting the adsorbed amount against the work of adsorption  $A$ . A curve fitting of all the data to the polynomial  $\ln(W) = a + b A$  was performed, where  $W$  is the volume of water adsorbed per unit adsorbent mass and  $(a, b)$  are fitting parameters. The best fit yielded  $a = -0.8797$  and  $b = -2.78 \times 10^{-4}$ , which is in good agreement with previously published values [18]. A considerable spread of about  $\pm 30\%$  with respect to this fit was found for the present data (Figure 7b).

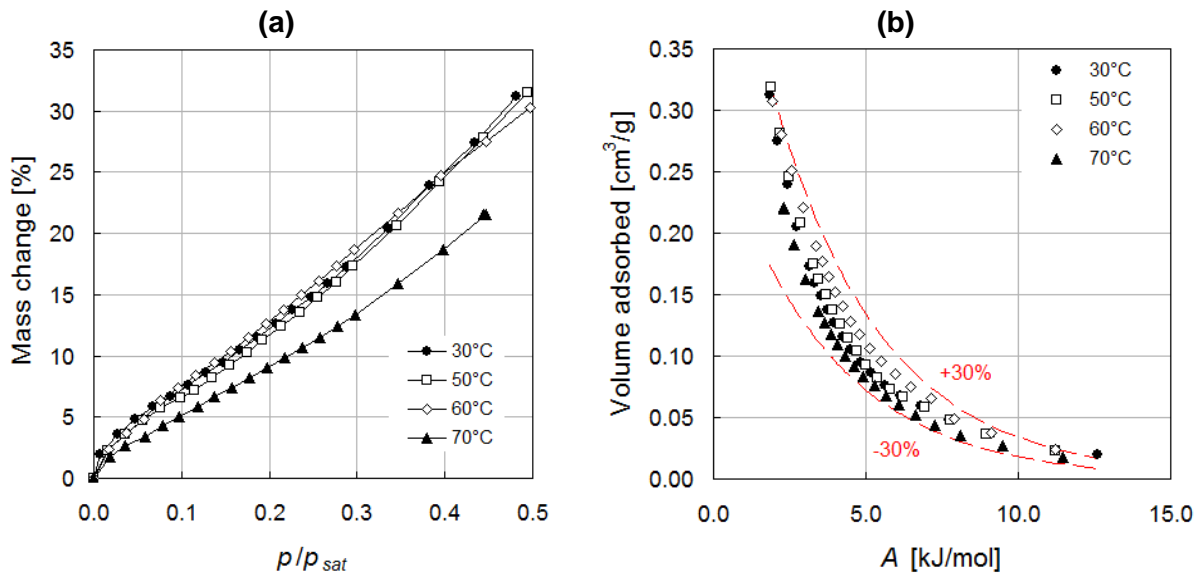


Figure 7: Water adsorption isotherms on Fuji RD silica gel (a) and corresponding volume adsorbed plotted against the work of adsorption  $A$

The temperature triples for the three adsorption cooling scenarios investigated in section 3.1 were transformed into  $(p/p_{sat})$ -values on the water adsorption isotherm measured at 50°C based on Equation (1). Thus, the thermodynamic maximum amount of water that can be cycled for each scenario is defined (Figure 8).

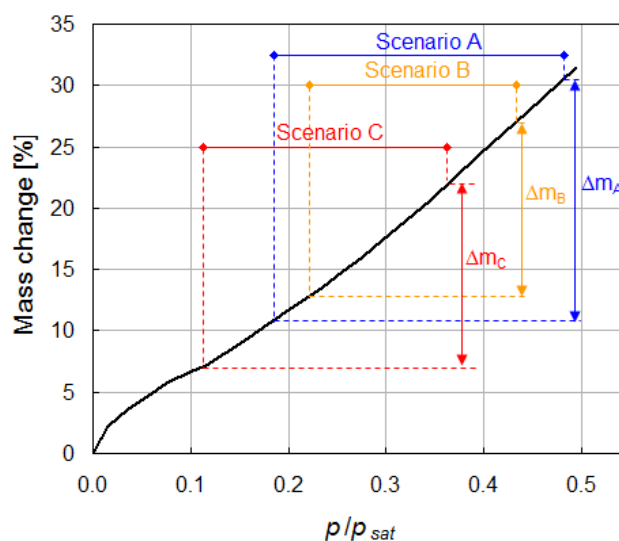
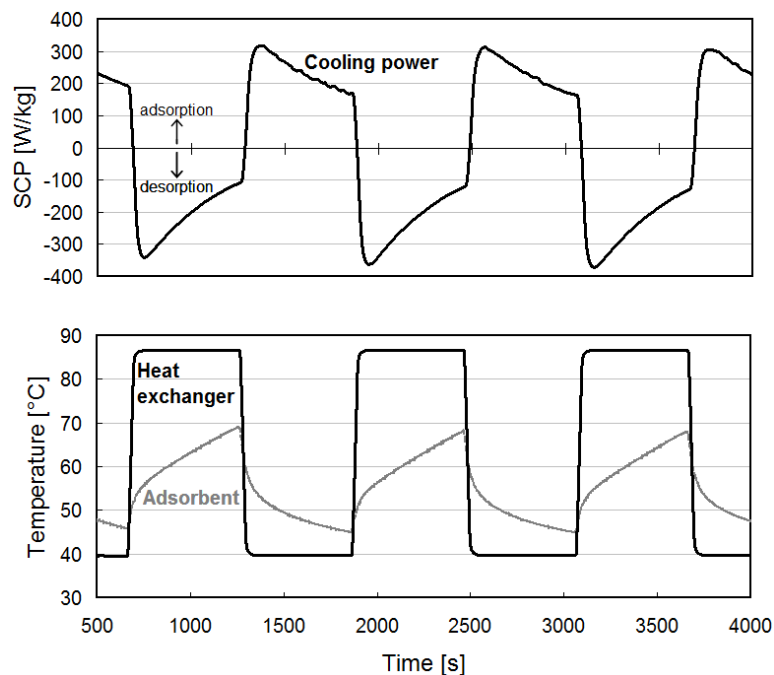


Figure 8: Water adsorption isotherm of Fuji RD silica gel at 50°C with corresponding thermodynamic operating windows for the three investigated adsorption cooling scenarios

The maximum possible amount of water cycled is  $\Delta m_A = 20$  wt% for Scenario A (Datacenter Munich),  $\Delta m_B = 14$  wt% for Scenario B (Datacenter Dallas) and  $\Delta m_C = 15$  wt% for Scenario C (Solar cooling Riyadh). Note that these cycling amounts are significantly smaller than the total water uptake capacity of the material near saturation ( $p/p_{sat} \rightarrow 1$ ), which is of the order of 40 wt%. Due to the approximately linear adsorption isotherm of Fuji RD silica gel, the adsorbent is able to cycle appreciable amounts of water within different  $p/p_{sat}$  windows. However, only less than half of the total adsorption capacity can be used in a typical application, which represents an ineffective use of the adsorbent material. The poor utilization of the adsorbent is reflected in the low  $COP_{th}$  values obtained by simulation of the three scenarios in Section 3.1.

The operating window of the adsorbent is narrowed even further due to incomplete thermal cycling. Figure 9 shows the cooling power and temperature excursions of the adsorber loaded with Fuji RD silica gel and cycled between temperature extremes of 90°C and 40°C at an evaporator temperature of 20°C (vapor pressure 23 mbar) with 10 minutes between switching events. The adsorbent temperature was derived from infrared thermography and represents an average value of the entire fixed bed. The specific cooling power goes through a maximum shortly after each switching event when the largest temperature gradient and hence driving force for adsorption is achieved during the experiment [19]. However, the temperature response of the adsorbent lags behind that of the heat exchanger significantly (Figure 9, bottom) due to the poor heat transfer between the heat exchanger and the silica gel and the poor thermal conductivity within the silica gel fixed bed itself.



**Figure 9: Specific cooling power (top) and temperature excursions of heat exchanger and adsorbent (bottom) of a tube-lamella heat exchanger loaded with Fuji RD silica**

From an adsorbent utilization perspective, it is favorable to employ long cycling times which result in higher  $COP_{th}$  for a given thermodynamic operation window. On the other hand, the SCP value decreases markedly with prolonged cycling time (Figure 9, top). Thus, cycling times for commercial adsorption chillers are selected close to the time for maximum SCP, but shifted to longer times to obtain improved  $COP_{th}$  values. For a commercial adsorption chiller utilizing silica gel/water as the working pair, a cycle time of 450 s has been reported [20]. It is obvious from Figure 9 that such short cycling times result in a significant reduction in the effective temperature swing of the adsorbent material. In fact, the actual change in the amount of water adsorbed for the cycling conditions in Figure 9 corresponds to ca. 5 wt% in

each cycle for the full 10 minutes cycling time. For comparison, the thermodynamic limit for the temperature triple {87°C, 40°C, 20°C} is 12.5 wt% based on Equation (1) and the adsorption isotherm of Fuji RD silica. Thus, there is a two-fold underutilization of the adsorbent in this case: (i) the operating boundary conditions only allow for a maximum utilization of ca. 31% of the total adsorption capacity of the adsorbent, and (ii) the poor thermal performance of the system further reduces the utilization of the adsorbent down to ca. 13% of the total adsorption capacity for a cycling time of 10 minutes. An improved adsorption cooling system in terms of adsorbent utilization, SCP and  $COP_{th}$  can be obtained by two main routes, namely the selection of an adsorbent material which specifically matches the boundary conditions of the application [21] or as process intensification through improvement of heat and mass transport within the adsorber heat exchanger [7].

#### 4 CONCLUSIONS

Adsorption cooling is attractive to make use of the vast pool of low-grade heat available from industrial processes or solar heat. Such utilization of otherwise unused heat reduces the primary fuel consumption and carbon footprint for air-conditioning and can help meeting the projected rise in global cooling demand while minimizing the imposed strain on power grids associated with vapor compression cooling. The implementation of adsorption cooling in datacenter applications with low-grade driving heat below 70°C is feasible to reduce or even eliminate the need for vapor compression cooling, thereby supporting server implementations with minimum overhead energy cost over their lifetime. Also, solar-driven cooling for residential air-conditioning is feasible even in regions with very high ambient temperatures, such as Saudi Arabia. Present adsorption cooling technology is limited in terms of efficiency and effectiveness due to the underutilization of the adsorbent materials in specific application scenarios. This was demonstrated experimentally in terms of the adsorption characteristics of widely employed micro-/mesoporous silica gel as well as the limited temperature swing undergone by a fixed-bed adsorber consisting of this adsorbent in a widely employed adsorber configuration. Advances in tailored adsorbent materials and enhancement of heat and mass transport within the adsorbent can boost the attractiveness of adsorption cooling for a wide range of industrial and residential applications.

#### 5 REFERENCES

- [1] International Energy Agency 2013, "Technology Roadmap: Energy efficient building envelopes."
- [2] Booz & Company 2012, "Unlocking the Potential of District Cooling: The Need for GCC Governments to Take Action."
- [3] Isaac, M., and Van Vuuren, D. P. 2009, "Modeling global residential sector energy demand for heating and air conditioning in the context of climate change," *Energy Policy*, Vol. 37, pp. 507–521.
- [4] U.S. Department of Energy 2008, "Waste Heat Recovery: Technology and Opportunities in U.S. Industry."
- [5] International Energy Agency 2012, "Technology Roadmap: Solar Heating and Cooling."
- [6] Núñez, T. 2010, "Thermally Driven Cooling: Technologies, Developments and Applications," *Journal of Sustainable Energy*, Vol. 1, pp. 16–24.

- [7] Critoph, R., and Zhong, Y. 2005, "Review of trends in solid sorption refrigeration and heat pumping technology," *Proceedings of the Institution of Mechanical Engineers, Part E: Journal of Process Mechanical Engineering*, Vol. 219, pp. 285–300.
- [8] Critoph, R. E. 1988, "Performance limitations of adsorption cycles for solar cooling," *Solar Energy*, Vol. 41, pp. 21–31.
- [9] Brunschwiler, T., Smith, B., Ruetsche, E., and Michel, B. 2009, "Toward zero-emission data centers through direct reuse of thermal energy," *IBM Journal of Research and Development*, Vol. 53, pp. 1–13.
- [10] Al-Mogbel, A., Ruch, P., Al-Rihaili, A., Al-Ajlan, S., Gantenbein, P., Witzig, A., and Michel, B. "The Potential of Solar Adsorption Air-Conditioning in Saudi Arabia: A Simulation Study," in *Proceedings of the 5th International Conference on Solar Air-Conditioning*, 2013, pp. 256–261.
- [11] Rasmussen, N. 2010, "Electrical Efficiency Modeling of Data Centers," *APC White Paper #113 Revision 2*.
- [12] Meyer, N., Ries, M., Solbrig, S., and Wettig, T. 2013, "iDataCool: HPC with Hot-Water Cooling and Energy Reuse," *Lecture Notes in Computer Science*, Vol. 7905, pp. 383–394.
- [13] IDC 2011, "Market Analysis Perspective: Worldwide Datacenter Trends and Strategies 2011."
- [14] Business Monitor International 2012, "Saudi Arabia Power Report Q1 2012."
- [15] Núñez, T., Mittelbach, W., and Henning, H. M. 2007, "Development of an adsorption chiller and heat pump for domestic heating and air-conditioning applications," *Applied Thermal Engineering*, Vol. 27, pp. 2205–2212.
- [16] <http://www.sortech.de>. [Accessed: 31-Jan-2014].
- [17] Dubinin, M. M. 1967, "Adsorption in Micropores," *Journal of Colloid and Interface Science*, Vol. 23, pp. 487–499.
- [18] Aristov, Y. I., Tokarev, M. M., Freni, A., Glaznev, I. S., and Restuccia, G. 2006, "Kinetics of water adsorption on silica Fuji Davison RD," *Microporous and Mesoporous Materials*, Vol. 96, pp. 65–71.
- [19] Aristov, Y. I. 2009, "Optimal adsorbent for adsorptive heat transformers: Dynamic considerations," *International Journal of Refrigeration*, Vol. 32, pp. 675–686.
- [20] Chua, H., Ng, K., Malek, A., Kashiwagi, T., Akisawa, A., and Saha, B. 1999, "Modeling the performance of two-bed, silica gel-water adsorption chillers," *International Journal of Refrigeration*, Vol. 22, pp. 194–204.
- [21] Aristov, Y. I. 2013, "Challenging offers of material science for adsorption heat transformation: A review," *Applied Thermal Engineering*, Vol. 50, pp. 1610–1618.